Influence of anomalous dispersion mirror properties on the quantum efficiency of InGaAs/GaAs resonant cavity photodetector

S.V. GRYSHCHENKO[a], STUDENT MEMBER, IEEE, A.A. DEMIN[a], STUDENT MEMBER, IEEE, I. A. SUKHOIVANOV[c], SENIOR MEMBER, IEEE, V.V. LYSAK[a,b], MEMBER, IEEE.

[a]*KHARKOV NATIONAL UNIVERSITY OF RADIO ELECTRONICS, KHARKOV, UKRAINE*
Fax: 380 57 7021 017 , e-mail: s_gryshchenko@kture.kharkov.ua
[b]*GWANGJU INSTITUTE OF SCIENCE AND TECHNOLOGY, GWANGJU, REPUBLIC OF KOREA*
[c]*UNIVERSITY GUANAJUATO, SALAMANCA, MEXICO*
Fax: 52 464 647 2400, e-mail: i.sukhoivanov@ieee.org

Abstract. *We present a theoretical analysis of the quantum efficiency of a resonant cavity enhanced InGaAs/GaAs P-i-n photodetector (PD) for the ultrashort optical connections. The numerical method of calculation of quantum efficiency combining a transfer matrix method and an energy conservation law is offered. Using anomalous dispersion (AD) mirror flattopped QE spectrum has been obtained. Conditions for ideal flattopped spectral response have been received. A design with a maximum QE of 93.5% and 3 nm bandwidth at 0.02 dB below the peak is presented.*

Key words: resonant-cavity enhanced photodetector, quantum efficiency, anomalous dispersion mirror, bandwidth.

1. Introduction

The progress in integrated circuits in past years shows that resonant cavity enhanced photodetectors are promising devises for optical interconnects [1], optical sensing applications, and could be used as receivers in ultrashort optical connections. Inserting a photosensitive active medium into Fabry-Perrot resonator results in enhanced quantum efficiency due to multiple reflections between mirrors [2]. As mirrors usually used distributed Bragg reflectors (DBRs), due to the high reflectivity. Resonant-cavity enhanced photodetector (RCE PD) possesses high speed operation and wavelength selectivity and is proper devise for data transfer systems [3]. The presence of the cavity leads to a narrow bandwidth (BW) determined first of all by cavity length and reflectance of mirrors. However, for the certain applications (e.g. high-speed telecommunications, optical interconnects and free-space communications) we require receivers with the broad-band flat-topped spectral response. Moreover, for application of the photodetector in bi-directional optical interconnects the successful decision of the cavity-mode misalignment problem is important. Even a slight mismatch of the cavity-mode wavelengths of paired VCSELs and RCE-PDs may considerably degrade the receiver sensitivity. Cavity-mode tuning method offered earlier [4] complicates fabrication of PDs, which can raise the production cost. Therefore, creation of the flat-topped quantum efficiency spectrum with as much as possible broad BW is an important task [5].

In this paper, we investigate an opportunity to create ideal flat-topped spectrum of a quantum yield using defect in periodic structure of the top mirror at fixed thickness and position of the active layer. We present the quantum efficiency spectra of the PD and their analysis for various numbers of layers in mirrors.

2. Formulations

The quantum efficiency (QE) of a PD is defined as the probability that single photon incident on the device generates an electron-hole pair which contributes to the detector current. We can determine total QE as a product of photon absorption probability η_a internal QE η_c and barrier collection efficiency η_b. Therefore:

$$\eta = \eta_a \cdot \eta_b \cdot \eta_c \,. \tag{1}$$

There exists two methods for calculation of the quantum efficiency of RCE PDs: analytical formulation [2], and semianalytical method [5]. In semianalytical method transfer matrix method (TMM) or based on final differences method is used for calculation of an electromagnetic field outside the active layer, and the analytical approach for calculation of the absorbed energy. The TMM is more flexible and accurate method for analysis periodic structures as RCE PD. However, in both methods the reflection at the interfaces between the emitter and intrinsic layers is ignored. Besides, from semianalytical models the standing-wave effect is excluded.

In the TMM the amplitude reflection r and transmission t coefficients are given by

$$r = \frac{\eta_m E_m - H_m}{\eta_m E_m + H_m} \tag{3}$$

$$t = \frac{2\eta_m}{\eta_m E_m + H_m} \tag{4}$$

where

$$\begin{pmatrix} E_m \\ H_m \end{pmatrix} = M \begin{pmatrix} 1 \\ \eta_s \end{pmatrix} \tag{5}.$$

η_{eff} represents effective refractive index of substrate or media and is give by

$$\eta_{eff} = \begin{cases} \dfrac{n}{\cos(\theta)} & \textit{for p-polarization} \\ n\cos(\theta) & \textit{for s-polarization} \end{cases} \tag{6}$$

E_m and H_m denotes respectively the electric and magnetic vectors in the incident medium, and M is a product matrix given by

$$M = M_L M_{L-1} \ldots M_j \ldots M_2 M_2 \tag{7}$$

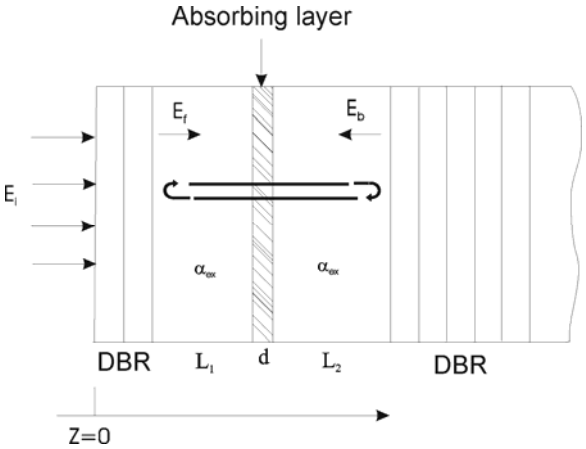

Fig.1 Schematic structure of conventional RCE PD

where M_j is a 2x2 matrix which represents the j-th film of the system [6]:

$$M = M * \begin{bmatrix} \cos(\delta) & \dfrac{i}{n_{eff}}\sin(\delta) \\ i * n_{eff} * \sin(\delta) & \cos(\delta) \end{bmatrix} \tag{8}$$

$$\delta_j = \frac{2*\pi}{\lambda}(n_j d_j \cos(\theta_j)) \tag{9}$$

The quantity $n_j d_j \cos(\theta_j)$ is the *effective* optical thickness of the layer j for an angle of refraction θ_j.

The quantum efficiency of RCE PDs can be calculated using reflection and transmission spectra using energy conservation rule, when we can neglect losses in mirrors and spacers. Absorption assigned by using complex refraction index $n_k = n - ik$ where k is the extinction coefficient. Extinction coefficient is the fraction of light lost to scattering and absorption per unit distance in a participating medium and defined as $k = \frac{\lambda\alpha}{4\pi}$, where α is absorption coefficient of material.

If we neglect the absorption outside absorption layer the quantum efficiency η_a is almost the same as the absorptance:

$$\eta_a = 1 - R - T \tag{11}$$

The quantum efficiency of RCE PDs can be calculated by reflection and transmission spectra when we can neglect losses in mirrors and spacers. From the energy conservation, meaning that the

absorption outside $In_{0.2}Ga_{0.8}As$ layer is negligible, the quantum efficiency, ηa, is almost the same as the absorptance A:

$$\eta_a = 1 - T - R \qquad (12)$$

Since TMM calculates the electric field distribution in the structure, the standing wave enhancement and the multi-reflections within the optical cavity, are inherently included. It should be noted that in our model, as well as in other models, it is neglected scattering and diffraction of light and considered only longitudinal distribution of waves. It is acceptable because normal incidence of light signals is assumed.

The barrier collection efficiency is given by [7]

$$\eta_b = \exp(-x / L_s), \qquad (13)$$

where L_s - scattering mean free path in the quantum well, made by image forces, x - distance from the barrier maximum to the interface.

Barrier collection efficiency was obtained from:

$$\eta_b = \exp(-x / L_z) \qquad (14)$$

where L_z denotes the inelastic scattering mean free path with a typical value of 200–300A [4].

The internal efficiency takes into account inelastic scattering in quantum wells of active region. The equation shows the probability of photoexcited carrier reach next layer.

$$\eta_c = \exp(-d / L_z) \qquad (15)$$

where d - quantum well thikness.

3. Investigated structures

The schematic of a $In_{0.2}Ga_{0.8}As/GaAs$ RCE PD is in Fig.2. $In_{0.2}Ga_{0.8}As$ absorbing layer is sandwiched between two GaAs spacer layers. For mature InP-based epitaxy technology, it is easy to grow a lattice constant matched InGaAs layer with a peak absorption wavelength at about 1.55 mkm. The top and the bottom mirrors are quarter-wave stacks of $Al_{0.65}Ga_{0.35}As/GaAs$ designed for high reflectance at 980nm center wavelength. Such mirrors are well known and can be easy fabricated with chemical vapor methods. Fig. 2a shows design with a λ/2-defect in top mirror leading to anomalous dispersion effect.

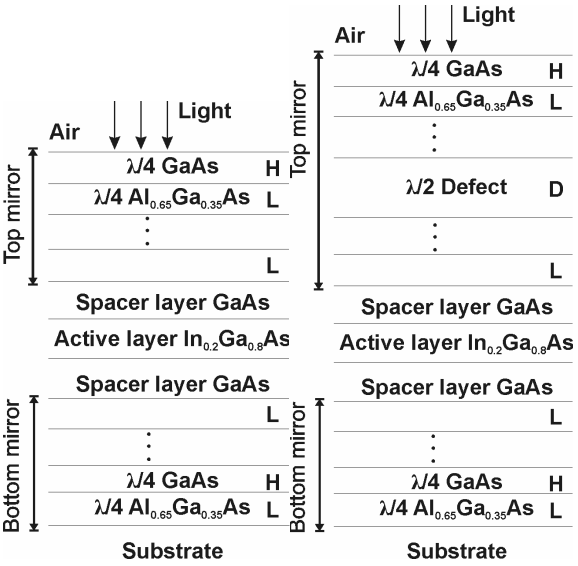

Fig.2. Schematic model of RCE PD. (a) shows scheme of a conventional RCE PD. (b) shows design with a λ/2-defect in top mirror leading to anomalous dispersion effect.

4. Results

Spectral responses of conventional RCE PD (grey curves) and RCE PD with defect in the top DBR (black curves) are presented in Fig. 3. Maximum of QE is at resonant wavelength that is connected first of all with the increased amplitude of the electric field inside a high-Q cavity.

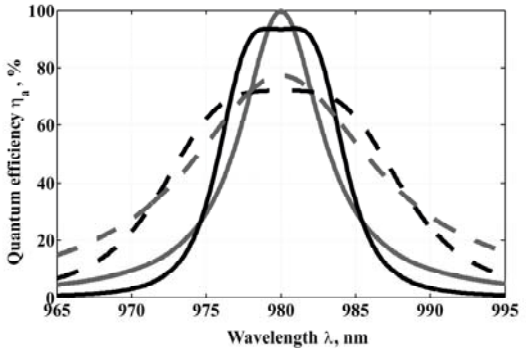

Fig. 3. QE spectra of RCE PDs. Grey curves illustrate results of simulation of conventional RCE PDs, where N1 = 8, N2 = 40.5 (solid curve); N1 = 3, N2 = 40.5 (dashed curve). Black curves illustrate results of simulation of RCE PDs with AD DBR, where p = 21, q = 4.5, N2 = 40.5 (solid curve); p = 15, q = 1.5, N2 = 40.5 (dashed curve).

Quantum efficiency can amount to 100% at the sufficiently large quantity of bottom mirror pairs (Fig. 4). As seen from the Fig 5, η decreases as $R2$ goes down at any value of $R1$.

The reason is that while decreasing $R2$, the losses increase considerably, as a part of radiation after every passage inside the resonator leaves it through the bottom mirror. Due to the small thikness of the efficient layer, the absorption per one passage is very small. Hence, the reflection coefficient of the bottom mirror should be as high as possible. Interesting moment is that the stronger the influence of the $R2$ magnitude on QE, the lower the absorption coefficient in the efficient layer (compare the curve bias in Figs. 3 and 4), as during one passage the ratio between the absorption in the efficient layer and the losses at the bottom mirror will become smaller [8,9].

The maximum QE occurs at following optimum reflection coefficient of the top mirror:

$$R1_{opt} = R2 \cdot \exp(-2\alpha_{eff} d_a), \qquad (16)$$

where R2 – the reflection coefficient of the

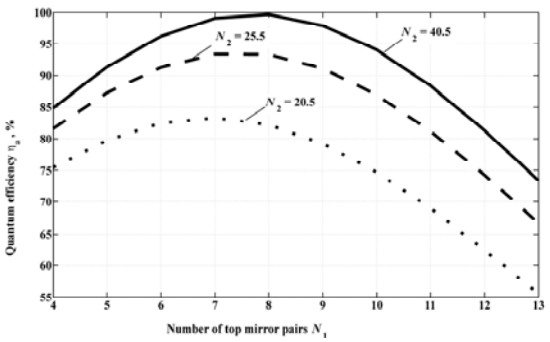

Fig. 4. Simulated QE of conventional RCE PDs versus the number of top mirror pairs N1 at different number of bottom mirror pairs N2.

bottom mirror, $\alpha_{eff} = \alpha \cdot SWE$ – the effective absorption coefficient in the active layer which considers the standing wave effect by factor SWE [2].Use of a mirror with anomalous dispersion of reflection phase as the top mirror allows to receive flat-topped spectral responses (black curves in Fig. 3) [5]. This effect can be explained in consideration of phase conditions in the resonator. Total change of phase in the cavity:

$$\Phi = \phi_C - \phi_1 - \phi_2, \qquad (17)$$

where ϕ_C - the phase taper during one round trip in the optical cavity, ϕ_1 - the reflection phase top mirror, ϕ_2 - the reflection phase bottom mirror.

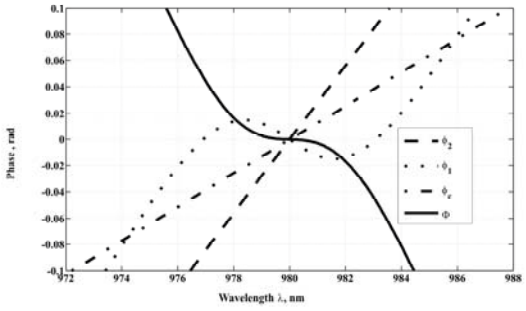

Fig. 5. Phases versus wavelength in RCE PD with AD DBR at $p = 21$, $q = 4.5$ and $N_2 = 40.5$.

Figure 6 presents wavelength dependences of phases shift in RCE PD with AD DBR ($p = 21$, $q = 4.5$ and $N_2 = 40.5$). The reflection phase of the top mirror changes is abnormal near to a resonance.

By changing number of layers in the top mirror, it is possible to achieve compensation of the phase variation of total phase caused by wavelength dependence ϕ_C and ϕ_2 in the certain wavelength range. In this wavelength range, a total phase Φ also $d\phi(\omega)/d\omega$ will be close to 0. The wavelength range in which the resonance of the inner electromagnetic field between the mirrors practically does not depend on wavelength meets the flat-topped range in Fig.3.

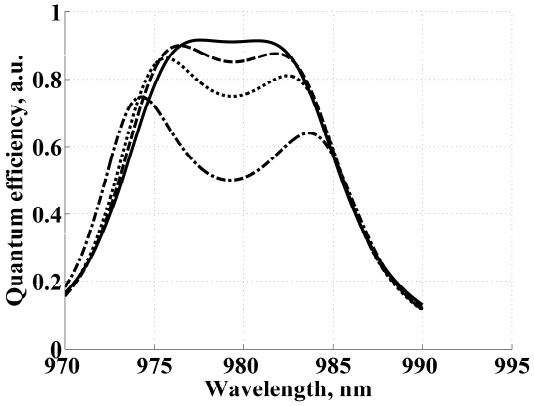

Fig 6 - Quantum efficiency spectrum. Solid curve corresponds to q=1.5, p=11. Dashed and dotted corresponds to q=2.5; 3.5 and 5.5 respectively.

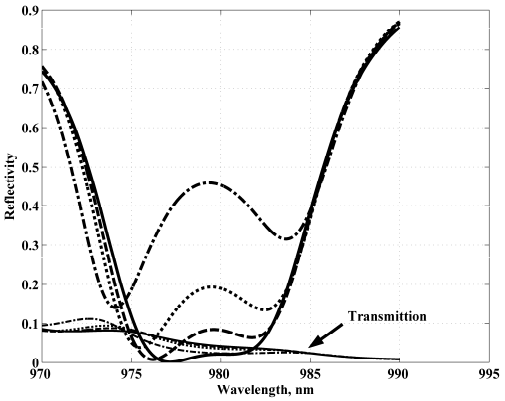

Fig 7 – Reflection spectrum. Solid curve corresponds to q=1.5, p=11. Dashed and dotted corresponds to q=2.5; 3.5 and 5.5 respectively.

Decreasing of QE value in the p = 15, q = 1.5 case results from lowering reflection coefficient of top mirror. From the other hand q = 1.5 decays spectral characteristics of AD microresonator. Therefore dashed curve still meets the flattop condition [10].

Figure 6 presents QE(η) wavelength dependence in RCE PD. Curves corresponds to the different p and q. p and q are the numbers of $Al_{0.65}Ga_{0.35}As/GaAs$ pairs and must satisfy p>q [3]. The main resonator and the resonator formed by AD layer have reflection minimum at the different wavelength (Fig. 7). Adding more layers to the top mirror (means increasing q) leads to narrowing bandwidth of the AD resonator. This effect provides increasing of the reflection between two cavity modes and decreasing the QE as a result. It should be noted that the transmitting characteristic does not change much due to high reflectance of the bottom mirror but such behavior of transmitting curve can be obtained only by neglecting absorption in dielectric mirrors.

Adding 2 mirror stack's will broke the flattop condition in the operating wavelength region and arising of 2 peaks. Simulation shows that mirrors can be designed so that QE spectrum will have 2 high and narrow peaks with a small distance between them. From figure 6, we can see that the maximum QE of 92.5% and 6 nm flattop width was obtained (solid curve).

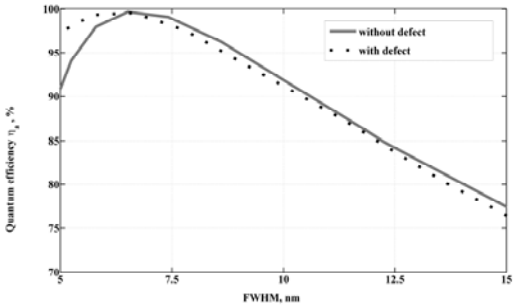

Fig. 8. Comparison of simulated QE versus FWHM of RCE PDs with AD DBR and conventional RCE PDs. As variables N_1, p and q were used.

It is of importance to note that FWHM is smaller in RCE PDs with half-wave defect in the top mirror, than it in conventional RCE PDs at identical QE (Fig. 8). It is connected with a steeper edge response for RCE PDs with AD DBR than that for conventional RCE PDs.

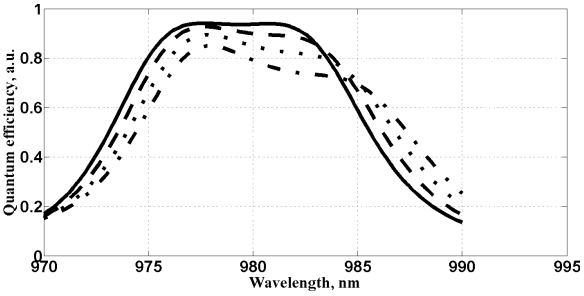

Fig. 9 Quantum efficiency spectrum. Solid curve d =100 nm, dashed d =105 nm, dotted d =110 nm, dot-dashed d =115 nm

On fig.9 we present result for different active layer thickness. The behavior of curves can be explained with understanding of reflection and transmitting characteristics changes again. Increasing of cavity media leads to a "red" shift of resonance wavelength. Decreasing QE amplitude results from increasing refraction coefficient on the non-resonant wavelength from one side and the InGaAs absorption coefficient dispersion from another[11]. The same characteristics was obtained while changing the spacer layers thickness.

4. Conclusions

Quantum efficiency for InGaAs/GaAs RCE PD was calculated by transfer matrix method and energy conservation conception. It has been shown that QE and bandwidth critically depend on cavity mirrors properties. By using an AD mirror in place of the DBR as top mirror we have achieved flattopped condition and high QE. Main factor for achievement flattopped the spectral response is the number of layers stack's of the top mirror denoted as p and q. This numbers can be used for definition of AD layer position in the mirror. Also the additional condition $d\phi(\omega)/d\omega = 0$ should be satisfied. A design with a maximum QE of 92.5% and 6 nm flattop width are presented. The presented design of the RCE PD is promising for optical interconnects applications and optical solutions in compute environment. It is shown that FWHM in RCE PDs with AD DBR it is no more, than it in usual RCE PDs because of steeper edge response.

Work is now proceeded with device optimization task While our results demonstrate flattoped QE spectrum, several issues need to be addressed in future work.

References

1. Zhou Y., Cheng J., Allerman A. A. High-speed wavelength-division multiplexing and demultiplexing using monolithic quasi-planar VCSEL and resonant photodetector arrays with strained InGaAs quantum wells. IEEE Photonics Technology Letters. 2000. Vol. 12, № 2, P. 122–124.
2. Unlu M. S., Strite S. Resonant Cavity enhanced photonic devices. J. Appl. Phys. 1995. Vol. 78, № 2. P. 607–639.
3. Liu K., Huang Y., Ren X. Theory and experiments of a three-cavity wavelength-selective photodetector. Applied Optics. 2000. Vol. 39, № 24. P. 4263–4269.
4. Chung I.- S., Lee Y. T. A method to tune the cavity-mode wavelength of resonant cavity-enhanced photodetectors for bidirectional optical interconnects. IEEE Photonics Technology Letters. 2006. Vol. 18, № 1. P. 46–48.
5. Chen C.- H., Tetz K., Fainman Y. Resonant-cavity-enhanced p-i-n photodiode with a broad quantum-efficiency spectrum by use of an anomalous-dispersion mirror. Applied Optics. 2005. Vol. 44, № 29. P. 6131–6140.
6. M. Bass, HANDBOOK OF OPTICS: volume I Fundamentals, Techniques, and Design. 2nd ed., McGRAW-HILL, INC., 1995.
7. Zhou Y., Cheng J., Allerman A. A. High-speed wavelength-division multiplexing and demultiplexing using monolithic quasi-planar VCSEL and resonant photodetector arrays with strained InGaAs quantum wells. IEEE Photonics Technology Letters. 2000. Vol. 12, № 2, P. 122–124.
8. S.V. Gryshchenko, A.A. Dyomin, V.V. Lysak, "Theoretical study of the quantum efficiency of InGaAs/GaAs resonant cavity enhanced photodetectors ", The International WORKSHOP on Optoelectronic Physics and Technology, P. 20-22, June 20-22, 2007 Kharkov, Ukraine.
9. S. V. Gryshchenko, A.A. Demin, V. V. Lysak "Quantum efficiency and reflection in resonant cavity photodetector with anomalous dispersion mirror",4-th International CONFERENCE on ADVANCED OPTOELECTRONICS and LASERS, September 29 - October 4, 2008, Alushta, Crimea, Ukraine.
10. S. V. Gryshchenko, A. A. Dyomin, V. V. Lysak, I. A. Sukhoivanov, "Optical absorption and quantum efficiency in the resonant-cavity detector with anomalous dispersion layer", 8th International Conference on Numerical Simulation of Optoelectronic Devices, 1 - 5 September 2008, University of Nottingham, United Kingdom.
11. Sadao Adachi, Physical properties of III-V, John Wiley & Sons, Inc., 1992.